GEM NEWS International

COLORED STONES AND ORGANIC MATERIALS

Amber with mineral inclusions. Besides its use as a gem material, amber has scientific value because of the wide variety of inclusions it contains. However, most such inclusions are organic in nature. Inorganic inclusions are rare, though pyrite and quartz have been reported (e.g., E. J. Gübelin and J. I. Koivula, *Photoatlas of Inclusions in Gemstones*, 2nd ed., ABC Edition, Zurich, 1992, pp. 212–228).

Recently, two transparent yellow samples (189.35 and 115.33 ct) with an unusually wide variety of inclusions—including some with a metallic appearance (figure 1)—were submitted to the NGTC Gem Laboratory for identification reports. Among the internal features were trapped insects, gas bubbles, reddish brown flow lines, plant debris, and minerals. Those with a metallic luster occurred in various sizes and shapes, and two were large enough to be seen with the unaided eye (again, see figure 1). With magnification, we observed a large number of round metallic inclusions, measuring several microns to several hundred microns, in one piece; a few reached the surface of the host and showed a "golden" metallic luster (figure 2). In the other sample, the metallic inclusions were interspersed with other minerals and organic material.

Figure 1. In addition to a variety of organic materials, these two samples of Baltic amber (189.35 and 115.33 ct) contain inclusions of pyrite and other minerals. Photo by Li Haibo.

The specimens fluoresced chalky blue to both long- and short-wave UV radiation, while the surface-reaching metallic inclusions were inert. Both samples had unpolished areas, making it easy to remove a minute amount of material for FTIR analysis. The spectra showed two characteristic peaks, at 1735 and 1157 cm^{-1}, indicating that the specimens were Baltic amber. Energy-dispersive X-ray fluorescence (EDXRF) spectroscopy of the metallic inclusions suggested pyrite, as both Fe and S were identified. The inclusions' Raman spectra showed two strong, sharp peaks at 372 and 339 cm^{-1}, with a weak peak at 425 cm^{-1}; these features are also characteristic of pyrite. Analysis of the other mineral inclusions in the 189.35 ct sample by Raman spectroscopy and microscopic examination between crossed polarizers identified them as feldspar, quartz, and jet (figure 3).

Editor's note: Interested contributors should send information and illustrations to Brendan Laurs at blaurs@gia.edu or GIA, The Robert Mouawad Campus, 5345 Armada Drive, Carlsbad, CA 92008. Original photos will be returned after consideration or publication.

GEMS & GEMOLOGY, Vol. 46, No. 4, pp. 309–335.

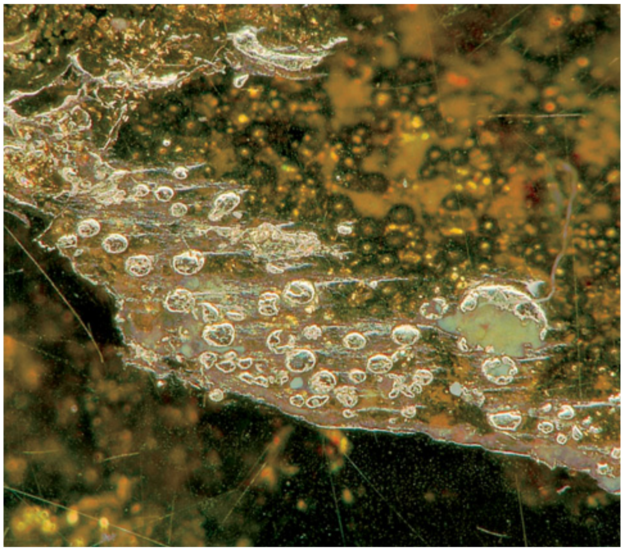

Figure 2. Where they reach the surface of the samples, the pyrite inclusions show a "golden" metallic luster. Photomicrograph by Li Haibo; magnified 100×.

In November 2010, a Burmese amber sample submitted to our laboratory displayed similar pyrite inclusions.

Li Haibo (lhb@ngtc.gov.cn), Lu Taijin, Shen Meidong, and Zhou Jun
National Gemstone Testing Center Gem Laboratory
Beijing, China

Additional field research on Tibetan andesine. In late September 2010, an international group investigated andesine occurrences in Tibet in an effort to resolve the controversy over the origin of red andesine from China. The group was organized by coauthor AA and hosted by miner Li Tong and his wife, Lou Li Ping. It also included Richard Hughes (Sino Resources Mining Corp., Hong Kong), Flavie Isatelle (geologist, France), Christina Iu (M. P. Gem Corp., Kofu, Japan), Thanong Leelawatanasuk (Gem & Jewelry Institute of Thailand, Bangkok), Young Sze Man (*Jewellery News Asia*, Hong Kong), and coauthor BML. The group flew from Guangzhou, China, to Lhasa, Tibet, and then drove west for ~7 hours (350 km) to Shigatse, Tibet's second-largest city. The andesine mining area is located about 1.5 hours' drive from Shigatse. Paved roads lead to within 1–3 km of all three reported Tibetan andesine localities: Bainang, Zha Lin, and Yu Lin Gu (see table 1 for GPS coordinates).

Figure 3. Microscopic examination of the larger amber sample between crossed polarizers reveals additional inclusions, composed of feldspar, quartz, pyrite, and jet. Photomicrograph by Li Haibo; magnified 100×.

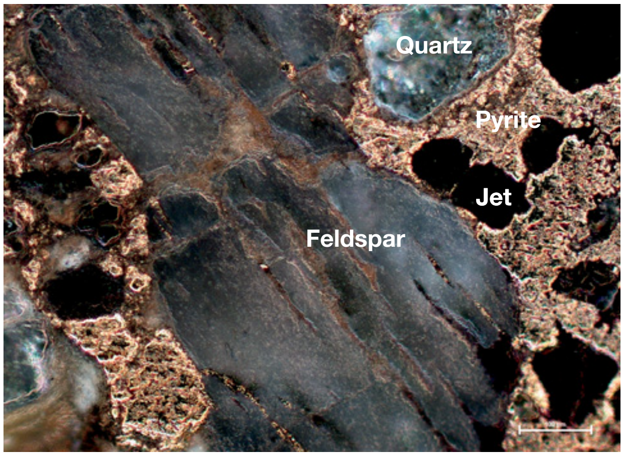

The Bainang mine, allegedly Tibet's principal source of andesine, was visited by one of us in 2008 (see Winter 2008 Gem News International, pp. 369–371; A. Abduriyim, "The characteristics of red andesine from the Himalaya highland, Tibet," *Journal of Gemmology*, Vol. 31, No. 5–8, 2009, pp. 283–298). The deposit is located ~2.2 km southwest of Nai Sa village, where we saw ~10 kg of material that local people claimed to have collected and stockpiled over the past three years. We were told most of the mining at Bainang took place in 2005–2008 and was organized by Li Tong. Unfortunately, we were forbidden from visiting the deposit by a powerful local lama, despite having official permission from the Chinese government and police escorts.

The Zha Lin deposit is located adjacent to a village of the same name. Reportedly it was mined by local people in 2006–2008 using simple hand tools, and ~2 tonnes of andesine were produced there. (Author AA did not visit the deposit in 2008 because Li Tong was not yet aware of it.) We saw a series of shallow pits in the mining area, but there was no evidence of recent digging. The deposit is hosted by medium-gray silty soil (figure 4, left) that underlies alluvial material consisting mainly of shale and mudstone with less-common quartz vein material. The authors dug two small pits (~0.7–1.2 m maximum depth) where we saw pieces of andesine on the surface, and many pieces were found at depth in both of them. We also dug three pits in random areas of alluvium (under thorn bushes) located 30–50 m upslope from the mining area where there was no surface evidence of andesine or prior digging (figure 4, right). These pits ranged up to 0.3 m deep, and andesine was found below the surface in two of them.

TABLE 1. Location of reported Tibetan andesine occurrences.

Location	GPS coordinates	Elevation
Bainang	29°02.48′N, 89°22.25′E (south mine)	4,100 m (13,452 ft.)
	29°02.72′N, 89°22.11′E (north mine)	4,076 m (13,373 ft.)
Zha Lin	29°03.95′N, 89°20.88′E	3,929 m (12,891 ft.)
Yu Lin Gu	29°03.08′N, 89°20.76′E	4,102 m (13,460 ft.)

Figure 4. Shallow pits dug in silty soil appear to be the source of andesine at the Zha Lin deposit (left). The site of one of the random test pits near Zha Lin from which the authors recovered andesine is shown on the right. Photos by B. M. Laurs.

As seen previously in andesine allegedly of Tibetan origin, all the rough material appeared waterworn and ranged from pale to deep red, with a few pieces containing bluish green areas.

At Yu Lin Gu, we found andesine scattered across an alluvial fan (figure 5) located ~2 km up-valley from Zha Lin. Reportedly ~200 kg of andesine have been collected there by local people since 2006, with no organized mining; the andesine has only been picked up from the surface. We collected several pieces that were locally concentrated in patches consisting of 4–10+ pieces per square meter. Most were found on raised portions of the dissected alluvial fan, and also in an active intermittent creek on one side of the fan. We recovered andesine from the surface or slightly below the surface in loose silty soil, but no stones were found when we dug pits into the alluvial fan. The range of color and degree of rounding in these pieces were similar to what was seen in the material from Zha Lin, but many were less saturated (figure 6).

We were unable to verify whether Yu Lin Gu is a true andesine deposit because we could not find samples at depth. At Zha Lin, our discovery of andesine within pits dug in random, previously unexplored areas near the reported mining area is consistent with what we would expect for a genuine Tibetan andesine deposit. The original source rock for the andesine was not evident in the area, and it may have eroded away. Our final conclusion regarding the controversies surrounding Tibetan andesine will depend on the laboratory analyses of samples obtained on this expedition.

Ahmadjan Abduriyim (ahmadjan@gaaj-zenhokyo.co.jp)
Gemmological Association of
All Japan – Zenhokyo, Tokyo

Brendan M. Laurs

Aquamarine and heliodor from Indochina. In June 2010, Jack Lowell (Colorado Gem & Mineral Co., Tempe, Arizona) informed GIA about some attractive gem-quality crystals of aquamarine and heliodor from Indochina (figures 7 and 8). According to his supplier (Tan Pham, Vietrocks.com, Philadelphia), good-quality aquamarine was mined in 2008 from northern Vietnam, from separate areas in the neighboring provinces of Thanh Hoa and Nghe An. The Thanh Hoa finds are located in Thuong Xuan District, while the Nghe An deposits are in Que Phong District. Aquamarine from Nghe An was also produced in 2003–2004; the more recent crystals range up to

Figure 5. At Yu Lin Gu, andesine was found on the surface of this alluvial fan. Photo by B. M. Laurs.

Figure 6. These andesines were recovered by the authors from the Zha Lin (left, 0.10–1.14 g) and Yu Lin Gu (right, 0.25–1.55 g) localities in Tibet. Photos by Robert Weldon.

20 cm long. Matrix specimens (associated with smoky quartz) have been recovered only rarely (from Thanh Hoa) due to the weathering of the pegmatite host rocks. Mr. Lowell indicated that the Thanh Hoa deposit has yielded substantially more production than Nghe An (specific data were unavailable), and that crystals from the latter deposit are a darker blue. Clean gemstones up to ~35 ct have been faceted from the Vietnamese aquamarine.

Well-formed crystals of heliodor (e.g., figure 8) were recently produced from another area in Southeast Asia, which Mr. Pham suspects is Cambodia. The crystals were first noted on the Vietnamese market with a third-party source in 2007; those seen by Mr. Pham ranged up to 7.5 cm long. This heliodor, as well as the aquamarine described above, has been popular with Chinese buyers.

Brendan M. Laurs

Figure 7. Fine aquamarine crystals such as these (up to 8.9 cm long) have been produced from a relatively new deposit in Thanh Hoa Province, Vietnam. Photo by Jack Lowell.

Dark blue aquamarine from Tsaramanga, Madagascar. In July 2009, 300 kg of dark blue aquamarine were recovered from a pegmatite at Tsaramanga, in central Madagascar.

Figure 8. These gem heliodor crystals (up to 7.5 cm long) are from Southeast Asia. Photo by Jack Lowell.

Figure 9. The Tsaramanga pegmatite mine in central Madagascar has produced notable finds of dark blue aquamarine in recent years. Photo by De Rosnay.

The mine (figure 9) is located 5 km from the village of Mahaiza, in the Betafo district. Tsaramanga was first mined by the Germans in the 1920s for tourmaline (black, yellow, and green), pink beryl, and other gem minerals. Today the main production is rose quartz from the pegmatite's core zone (figure 10, left), but occasional concentrations of large (up to 1.5 m long and 40 cm in diameter) dark blue aquamarine crystals are uncovered (e.g., figure 10, right). Some beryls showing multiple colors have also been discovered, though not of gem quality.

The geology of the area consists of gabbros that are intruded by feldspar-rich pegmatites and some large veins of quartz. There are two types of pegmatites, defined by their mica content: muscovite bearing (with aquamarine) and biotite-phlogopite bearing. The main open pit at Tsaramanga measures ~70 × 20 m, and is worked by a team of 10–12 miners using pneumatic drills and hand tools such as hammers and steel bars.

About 10% of this recent aquamarine production was facetable, while 60% was cabochon and carving grade, and the remaining material was fractured and opaque. The unusually dark color of the aquamarine makes this mine noteworthy. Although the kilogram-size beryl crystals (e.g., figure 11) are highly fractured due to their formation within quartz and feldspar rather than open pockets, they typically contain substantial gemmy areas (figure 11, inset) that can yield attractive faceted stones up to ~6–7 ct.

Flavie Isatelle (flavie.isatelle@gmail.com)
Avignon, France

Diopside from Pakistan. In 2007, gem dealer Farooq Hashmi (Intimate Gems, Jamaica, New York) obtained a parcel of pale yellowish green rough in Peshawar, Pakistan. The seller indicated that it was from a new find in the Northern Areas of Pakistan (now called Gilgit-Baltistan), but he did not know the identity of the material. The 200 g parcel contained pieces weighing ~1–5 g. Mr.

Figure 10. The main pit at Tsaramanga (left) is mined primarily for rose quartz, but occasional concentrations of large dark blue aquamarine crystals (right) have been discovered. Photos by F. Isatelle

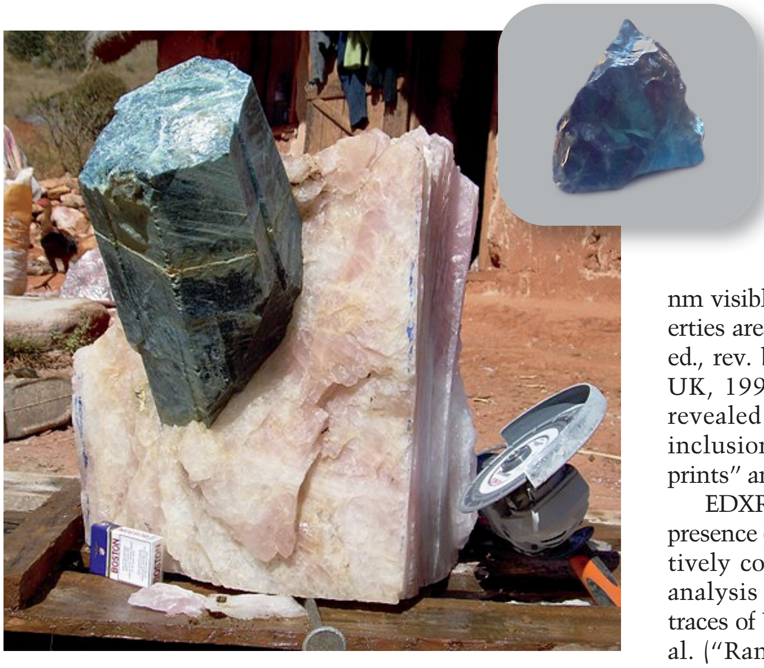

Figure 11. This specimen of aquamarine in rose quartz matrix shows the unusually dark color of the material from Tsaramanga. Such crystals typically contain abundant fractures with small gem-quality areas (see inset). Photos by De Rosnay.

Hashmi saw another parcel of this material with the same dealer during a subsequent trip in mid-2008, but it was of inferior quality.

Mr. Hashmi loaned GIA two well-formed crystals and a 1.97 ct round brilliant, faceted by Robert Buchannan (Hendersonville, Tennessee; see the *G&G* Data Depository at gia.edu/gandg for faceting notes), which are shown in figure 12. Standard gemological testing gave the following properties: color—light yellowish green to yellowish green; pleochroism—none; RI—n_α = 1.670–1.675 and n_γ = 1.695–1.698; birefringence—0.025–0.028; hydrostatic SG—3.27; Chelsea filter reaction—none; fluorescence—inert to long- and short-wave UV radiation; and a fine absorption line at 505 nm visible with the desk-model spectroscope. These properties are consistent with diopside (R. Webster, *Gems*, 5th ed., rev. by P. G. Read, Butterworth-Heinemann, Oxford, UK, 1994, pp. 330–331). Microscopic examination revealed strong doubling in the faceted stone (and no inclusions), while the two crystals contained "fingerprints" and iron-stained fractures.

Figure 12. These three samples (the round brilliant weighs 1.97 ct), reportedly from northern Pakistan, proved to be diopside. Photo by Robert Weldon.

EDXRF spectroscopy of the three samples showed the presence of Si, Mg, Ca, Fe, Al, and Cr. Laser ablation–inductively coupled plasma–mass spectrometry (LA-ICP-MS) analysis indicated a similar composition and revealed traces of V. Previous research on pyroxenes by E. Huang et al. ("Raman spectroscopic characteristics of Mg-Fe-Ca pyroxenes," *American Mineralogist*, Vol. 85, 2000, pp. 473–479) confirmed that Raman spectroscopy can differentiate diopside from other minerals in the (Mg,Fe,Ca)-pyroxene group, such as enstatite, ferrosilite, hedenbergite, and wollastonite. The Raman spectra of these three samples showed diopside vibration modes similar to those published in Huang et al. (spectra are available in the *G&G* Data Depository). We therefore identified the material as diopside.

Pamela Cevallos (pcevallo@gia.edu)
GIA Laboratory, New York

Record-breaking emerald discovered in Hiddenite, North Carolina. Although the area around Hiddenite, North Carolina, has historically produced some exquisite mineral specimens, gem-quality emeralds from this localitiy are exceedingly rare and highly sought-after by collectors. Until recently, the largest known faceted example was an 18.88 ct pear shape, named the Carolina Queen. The ~14 g rough from which it was cut was found in the fall of 1998 at the Rist mine, now called the North American Emerald mine. This same crystal also produced a 7.85 ct oval named the Carolina Prince, which sold for $500,000 to a collector with family ties to the town of Hiddenite.

In August 2009, a 62.01 g gem-quality emerald crystal was discovered in decomposed soil at the Adams Farm (figure 13), previously known primarily as a source of hiddenite (green Cr-bearing spodumene). Miner Terry Ledford and landowner Renn Adams unearthed the emerald from a depth of 4.3 m while pursuing the seams that occasionally lead to pockets containing hiddenite. The discovery occurred in an open field near an overgrown exploration site originally developed by Dr. William Hidden, who was reportedly dispatched to the area by Thomas Edison to procure platinum for his light bulb filaments. Together Dr. Hidden and Dr. George Frederick Kunz—the well-known late 19th/early 20th century gemologist-author—identified

Figure 13. Miner Terry Ledford displays the large emerald crystal next to the pocket where it was found in August 2009 in Hiddenite, North Carolina. The crystal (inset) was well formed and weighed 62.01 g. Photos courtesy of Terry Ledford.

63 different gems and minerals in the Hiddenite area.

The rough emerald exhibited rutile crystals on some faces, a classic signature of North Carolina emerald. After several weeks of study, the owners decided to cut the largest gem possible and enlisted the services of Jerry Call, an experienced cutter who had also faceted the 13.14 ct pear-shaped Carolina Emerald acquired by Tiffany & Co. in the 1970s. The result was a free-form step cut that weighed an impressive 74.66 ct, a new North American record.

Figure 14. The recut emerald, named the Carolina Emperor, is shown with an enlarged image of the 60+ ct Catherine the Great Emerald brooch on the cover of this Christie's catalog dated April 22, 2010. Photo by C. R. Beesley.

Soon after, Christie's announced the sale of a 60+ ct Colombian emerald brooch that belonged to Russia's Catherine the Great in the 18th century. Because of the size and quality similarities between the two emeralds, Adams and Ledford agreed with the suggestion to recut their stone into a hexagonal mixed cut emulating the Catherine the Great Emerald (figures 14 and 15). After three days of meticulous recutting by Ken Blount of Nassi & Sons, in New York City, the recut gem weighed 64.83 ct and showed a significant improvement in appearance. Dubbed the Carolina Emperor, it is the largest cut emerald from North America and has set a new benchmark for size and quality of North Carolina emeralds.

C. R. "Cap" Beesley (capbeesley@yahoo.com)
Gemstone Standards Commission, New York City

Figure 15. At 64.83 ct, the Carolina Emperor is the largest cut emerald from North America. Photo by C. R. Beesley.

Figure 16. Attractive cabochons of emerald-in-matrix (here, 15.27 and 34.37 ct) have recently been produced from material mined in Bahia, Brazil. Photo by Robert Weldon.

Emerald-in-matrix from Bahia, Brazil. At the 2009 Tucson gem shows, Joseph Rott (Tropical Imports, Belo Horizonte, Brazil) informed GIA about polished samples of emerald-in-matrix that were sourced from a long-known emerald deposit in Bahia, Brazil. This material consists of euhedral translucent emerald crystals embedded in white (or rarely pale pink) feldspar. Similar material has been reported from the Big Crabtree mine in Mitchell County, North Carolina (Summer 1993 Gem News, p. 132), and from the Nova Era area of Minas Gerais, Brazil (Summer 2002 GNI, pp. 176–177).

Mr. Rott donated two square cabochons of the Bahia material to GIA (figure 16), and they were studied for this report. The white matrix was confirmed to be feldspar and quartz by Raman analysis. EDXRF spectroscopy indicated that chromium (rather than vanadium) was the chromophore in the emerald. The cause of color in the pale pink feldspar was explored with EDXRF but could not be determined conclusively. Examination of the samples with magnification revealed inclusions of feldspar and dark brown mica (identified by Raman analysis as biotite); the emeralds also showed fracturing throughout. As with many emeralds, these samples were clarity enhanced by oiling. The oil was easily visible when tested with a hot point, as the fractures began to sweat slightly. The fractures in the samples fluoresced moderate blue to long- and short-wave UV radiation, which also provides evidence of clarity enhancement.

Mr. Rott indicated that ~100 kg of this material has been mined and over 2,000 carats of cabochons have been cut in sizes ranging from 8 × 10 mm to 20 × 25 mm. This emerald-in-matrix offers another option for designers, collectors, or anyone else who appreciates new and unusual gem materials.

Nathan Renfro (nrenfro@gia.edu)
GIA Laboratory, Carlsbad

5th century garnet jewelry from Romania. In 2007, nine gold pendants were discovered in an ancient tomb excavated at a shopping center 5 km west of Cluj-Napoca, Romania. Archeologists determined that the pieces belonged to a princess of the 5th century Gepids, a Gothic tribe (contemporaneous with the Merovingians) who lived in the Transylvania region of central Romania. Each pendant measured ~3.85 cm long and contained five tablet-cut red stones (about 1.5 mm thick) in a closed-back setting (figure 17). Their initial appearance suggested they were rubies. The jewels were studied on a single day using nondestructive techniques, and the results were initially presented at the XIX Congress of the Carpathian-Balkan Geological Association in Thessaloniki, Greece, in September 2010.

The stones were isotropic, with a refractive index of ~1.78 (using the spot method on the edge of one slab that protruded from the mounting), and had an almandine-like spectrum. Each plate contained crystallographically oriented rutile needles, and some of the plates contained pinpoints, negative crystals, and small crystals with the appearance of apatite. Most prominent were black, sometimes hexagonal, platy crystals (figure 18) that were nearly identical to ilmenite inclusions seen previously in almandine (see, e.g., E. J. Gübelin and J. I. Koivula, *Photoatlas of Inclusions in Gemstones*, 3rd ed., ABC Edition, Zurich, 1997, p. 289). Raman spectroscopy confirmed the stones were garnet with a high almandine content, with main bands at ~915, 550, 500, and 350 cm^{-1}.

EDXRF spectroscopy showed the metal was nearly pure gold, with only traces of Ag and Cu. A crisscross waffle-like pattern was stamped into gold foil mounted in the gold setting behind the garnet slices (see figure 19). This texture was visible through the transparent stones, producing an effect reminiscent of modern guilloché enamel, in which a pattern is engraved in the metal before the enamel is applied. A similarly stamped foil configuration has been observed in garnet, silver, and gold jewelry from nearby Potaissa, also a Gepid site (C. Ionescu and V. Hoeck, "Zusammensetzung und Herkunft der Granate der Ohrringe und einer Gürtelschnalle aus dem Grab der Franziska aus Potaissa [Turda, Rumänien] [About the composition and origin of garnets mounted in the earrings and buckle from the tomb of Franziska in Potaissa (Turda, Romania)]," in M. Barbulescu, Ed., *Das Germanische Furstengrab von Turda* [*The Germanic Princess Tomb from Turda*], Tribuna, Cluj-Napoca, Romania, 2008, pp. 295–310).

The almandine-rich composition of this garnet would be expected to have an overdark appearance if such material was faceted into stones of typical size for jewelry. Its use in these pendants was possible only because the plates are so thin. Generally, red gem garnets are a mixture of pyrope and almandine, with typically >40% pyrope (see figure 7 of D. V. Manson and C. M. Stockton, "Gem garnets in the red-to-violet color range," Winter 1981 *G&G*, pp. 191–204). The flat morphology of the garnet plates may have resembled the shape of the original rough if the crys-

Figure 17. These 5th century gold and garnet pendants (~3.85 cm long) were discovered near Cluj-Napoca, Romania. Photo by C. Ionescu.

tals had developed "fracture cleavage," as described by J. Ganguily et al. ("Reaction texture and Fe-Mg zoning in granulite garnet from Søstrene Island, Antarctica: Modeling and constraint on the time-scale of metamorphism during the Pan-African collisional event," *Proceedings of the Indian Academy of Sciences, Earth and Planetary Sciences*, Vol. 110, No. 4, 2001, pp. 305–312). Although our research is ongoing, we believe the garnet originated from European deposits that were known at the time, possibly the Austrian localities of

Figure 18. Several inclusions were visible in the garnet slices, including black platy crystals of what appeared to be ilmenite. Photomicrograph by C. Ionescu; field of view ~2.7 mm.

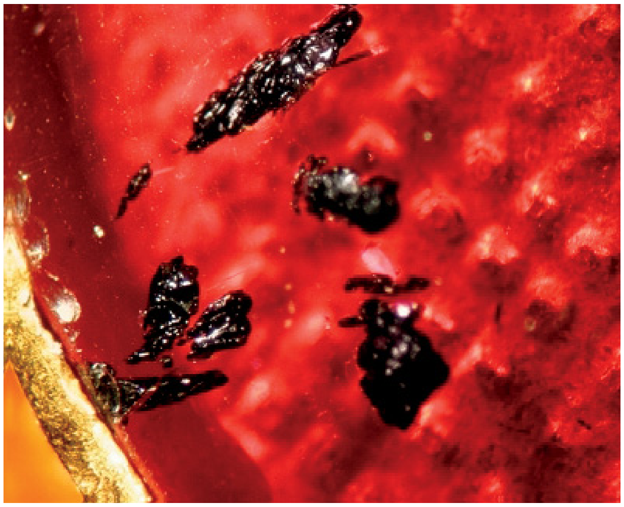

Figure 19. Each flat almandine slice is set above a crisscross-stamped piece of gold foil. The appearance is reminiscent of guilloché enamel. The foil contains a few square holes that were probably produced during the stamping process. Photomicrograph by C. Ionescu; field of view ~2.7 mm.

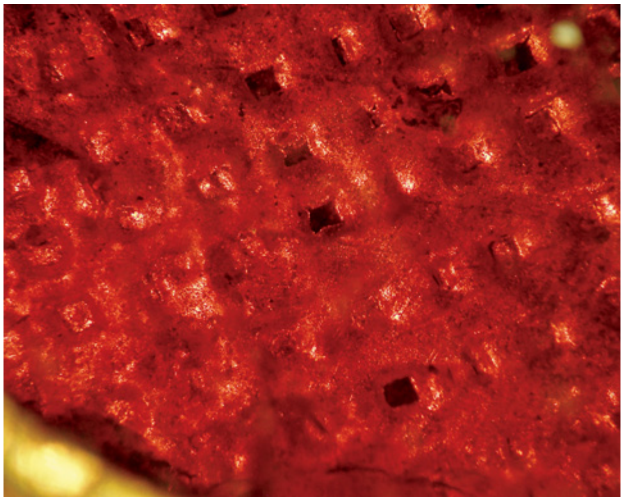

Figure 20. Shown here are some of the Pinctada radiata *and pen shells collected during a recent dive off the coast of Bahrain. The largest shell is ~50 cm long. Photo by A. Al-Attawi.*

Dunkelsteinerwald or Zillertal.

Acknowledgment: This study was funded by the Romanian Ministry of Education and Research, ID-2241/2008.

Emmanuel Fritsch

Corina Ionescu (corina.ionescu@ubbcluj.ro),
Viorica Simon, Szabolcs Nagy,
Katalin Nagy-Póra, and Mihai Rotea
Babes-Bolyai University, Cluj-Napoca, Romania

Figure 21. A near-"golden" off-round pearl (5.0–5.5 mm) was found in this P. radiata *oyster. Photo by A. Al-Attawi.*

Natural pearl diving off the coast of Bahrain. In June 2010 while visiting Manama, Bahrain, these contributors had an opportunity to experience pearl diving in a manner similar to that used in the past. Although our methods were not completely authentic in a historic sense—that is, no nose clip (*Al Fetam*), no stone weight (*Al Kher*) to take us to the sea bed, no person on deck to pull the rope attached to the net basket and accompanying diver to the surface (*Al Seib*), no net bags (*Al Deyeen*) to contain the shells collected on the sea bed, and no traditional fishing vessel (e.g., dhow)—we did search for mollusks without using compressed air.

Our first stop was an area southeast of Manama's Marina Club (~45 minutes by boat) that had been recommended by local contacts. The water was just over 2 m deep, and the sea bed was liberally scattered with specimens of *Pinctada radiata* and some Pinnidae ("pen shell") bivalves (~5–10 shells/m^2). We collected shells of both mollusks before moving to a slightly shallower area nearby. Although that area contained <5 shells/m^2, it did not take long to collect ~200 shells total, mostly *P. radiata* but also some pen shells (e.g., figure 20).

On the boat trip back to Manama, we opened the mollusks with knives and carefully examined their interiors for pearls. Contributor AA-A discovered an ~2 mm cream-colored seed pearl in the mantle region of a *P. radiata*, and contributor AA found a 5.0–5.5 mm near-"golden" pearl within the gonad region of a *P. radiata* (figure 21). Two small blister pearls were also found attached to shells.

Only two whole pearls were found in the 200 or so mollusks recovered. This 1:100 ratio provides some idea of how many Arabian Gulf oysters must be opened to find a pearl worthy of mention, a notion that was reinforced by

Figure 22. Quantities of fine natural pearls are still being produced in the Arabian Gulf. The largest shown here is ~10 mm. Courtesy of Al-Mahmood Pearls; photo by N. Sturman.

several dealers in Manama. Nevertheless, it is significant that the Arabian Gulf still produces natural pearls (e.g., figure 22).

Nick Sturman (nsturman@gia.edu)
GIA Laboratory, Bangkok

Stefanos Karampelas
Gübelin Gem Lab, Lucerne, Switzerland

Ali Al-Attawi
Gem & Pearl Testing Laboratory of Bahrain, Manama

Ahmadjan Abduriyim

Update on ruby and sapphire mining in Pakistan and Afghanistan. In June–July 2010, this contributor visited two corundum deposits in Pakistan and Afghanistan to collect reference samples for GIA: Basil in Pakistan and Jegdalek in Afghanistan.

In Pakistan, ruby and sapphire have been reported from five deposits: Nangimali (in Pakistan-controlled Azad Kashmir), Hunza (in northern Pakistan along the Karakorum Highway; see, e.g., Fall 2007 GNI, pp. 263–265), Bisil (in northern Pakistan's Basha Valley; see Fall 2007 GNI, pp. 263–265), Basil (in the Kaghan Valley of North-West Frontier Province), and Batakundi (also in the Kaghan Valley, located 30 km from Basil). Regarding the Bisil deposit, this author was unable to confirm its existence or learn any information about the activity there.

The Basil deposit was discovered in 1996. There were three mining sites as of June 2010, operated by Kashmir Gems Ltd. (e.g., figure 23). The first two produce pink, purple, and blue sapphires from graphite veins. At the third site, pink sapphires are found associated with marbles. Mining usually takes place from June to October by small teams using explosives and jackhammers. The output (e.g., figure 24, left) appears to be more significant than that of Nangimali or Batakundi. From this author's field research and conversations with miners/dealers who worked in Batakundi for several months in 2003 and 2004, it turns out that Basil is the source of the pink-to-purple sapphires previously described as coming from Batakundi (see Winter 2004 GNI, pp. 343–344; www.gia.edu/research-resources/news-from-research/batakundi_sapphire.pdf). By contrast, Batakundi is the source of distinctly different material (e.g., figure 24, right) and is more difficult to access. According to Guy Clutterbuck (pers. comm., 2006), Batakundi began producing small dark red rubies from a marble-type deposit in 2000, but several miners apparently died as a result of falls or from altitude sickness. Mining at

Figure 23. Pakistani miners are seen at the entrance of a sapphire mine in Basil, Pakistan. The mine is located at an altitude of 4000 m. Photo by V. Pardieu.

Figure 24. Some rough and faceted (~0.7 ct) sapphires from Basil are shown on the left. On the right are rubies reportedly from Batakundi, Pakistan; the smaller stones are 0.4–1 ct. Photos by V. Pardieu.

Figure 25. The pieces of rough in this parcel of blue sapphires from Badakhshan weigh up to 4 g. Photo by V. Pardieu.

Batakundi is said to have stopped after the devastating earthquake that hit Azad Kashmir in September 2005.

In Afghanistan, there are four ruby and sapphire deposits. Jegdalek, located in the eastern part of Kabul Province near Sorobi, is a well-known source of ruby from a marble-type deposit (G. W. Bowersox et al., "Ruby and sapphire from Jegdalek, Afghanistan," Summer 2000 *G&G*, pp. 110–126). The mining area is about 10 km long by 2 km wide and operates year-round. Approximately 200–300 miners were working the area in July 2010, significantly more than during this contributor's visit in the summer of 2006 (when mining was illegal). Ruby-bearing marble is dug from trenches extending over several hundred meters, and some tunnels are reportedly more than 200 m deep. According to the miners, output is limited by a lack of explosives, and water infiltration is a problem in some deep trenches.

Near Maidan Shar, in Vardak Province, a small blue sapphire deposit was active at the beginning of the 2000s (Winter 2004 GNI, pp. 343–344), but mining reportedly stopped because there was no market for the stones. The material was too gray and included, and treatments were not effective in improving it. The deposit reportedly closed after 2006.

In Badakhshan Province, a small marble-hosted ruby deposit is supposedly located near Khash (see Fall 2007 GNI, pp. 263–265), a small village about two hours west of the village of Bohorak. In July 2010 this author was not allowed to come within 1 km of the reported deposit. Fewer than 10 miners were said to be working in tunnels dug on a hillside overlooking the valley. According to local residents, besides rubies and some low-quality blue sapphires, the area around Bohorak and the village of Jorm produces blue spinel, sphene, aquamarine, green and pink tourmaline, and diopside.

Also in Badakhshan, blue sapphires were reportedly discovered in 2008 near the famous lapis lazuli mines at the village of Sar-e-Sang. The sapphires are associated mainly with mica, and usually form hexagonal bipyramidal crystals that range up to 4 g (figure 25). Dealers in Kabul reported that the main market for these sapphires is Jaipur, India.

Chicken Street, the main gem trading area in Kabul, was much more active in 2010 than in 2006. Rubies were available from Jegdalek as well as Tajikistan, and some parcels also contained synthetics and heated stones (probably of African origin). Lead glass–filled rubies were also common in the Kabul market. Also seen were many parcels of emeralds said to be from Panjshir and Laghman (Afghanistan), Xinjiang (China), Swat (Pakistan), and Zambia. Afghan tourmaline, kunzite, and aquamarine (reportedly from Kunar and Nuristan), and pink spinel from Tajikistan, were also available in a variety of quantities and qualities.

Vincent Pardieu (vpardieu@gia.edu)
GIA Laboratory, Bangkok

Figure 26. These sapphires were found in 2009 in the Auvergne region of central France. Photo by B. Devouard.

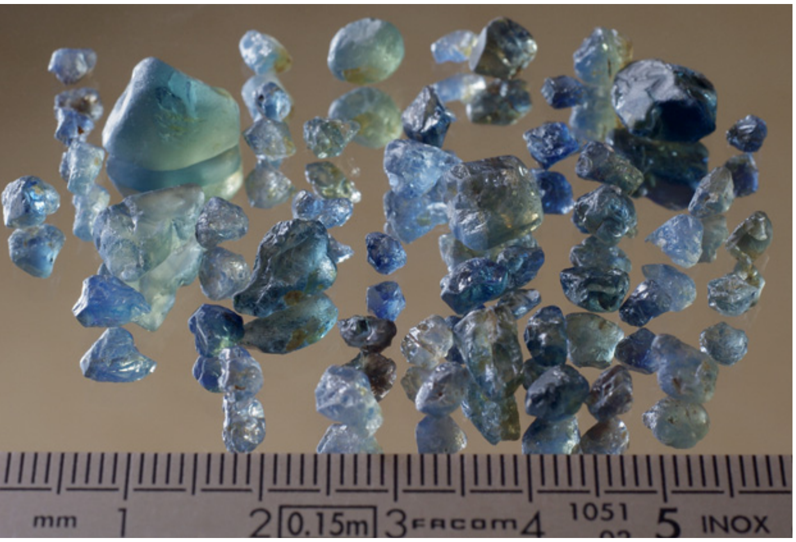

Figure 27. These faceted sapphires from the Auvergne discovery range from 0.3 to 5.0 ct. Photo by B. Devouard.

Figure 28. This sapphire washing area lies near the village of Ambalavy, about 50 km southwest of Ilakaka. Photo by V. Pardieu.

Rediscovery of sapphires in central France. The Auvergne region, in France's Massif Central, was an important source of gems from the Middle Ages to the end of the 19th century (F. H. Forestier, "Histoire de l'un des gisements de gemmes le plus anciennement connu d'Europe occidentale: Saphirs, grenats et hyacinthes du Puy-en-Velay [History of one the oldest known gem deposits in western Europe: Sapphires, garnets, and zircons from Puy-en-Velay]," *Cahiers de la Haute Loire*, 1993, pp. 81–152). This region has been affected by several episodes of Cenozoic volcanism that resulted in abundant alkaline basaltic flows. In 2009, a prospector panning a riverbed found several thousand carats of rough sapphires. The stones ranged from 2 to 15 mm and had irregular resorbed shapes, with colors ranging from greenish yellow to greenish blue to saturated blue, as well as dark blue and black. Their moderate-to-strong pleochroism was typical of magmatic sapphires from basaltic terrain.

Approximately 10% (~40 g) of the rough was of gem quality (e.g., figure 26), and a dozen stones have been faceted (e.g., figure 27) by lapidary Jacques Dreher in Clermont-Ferrand, the regional capital. These gems weighed 0.3–5.0 ct and were mostly clean to lightly included. Gem-quality sapphires in such quantity and quality have not been encountered in France, or arguably all of Europe, since the workings at Mont Coupet (also in Auvergne) during the late 19th century.

Bertrand Devouard (b.devouard@opgc.univ-bpclermont.fr) and Etienne Médard
Laboratoire Magma et Volcans, Blaise Pascal University
CNRS (UMR 6524), Clermont-Ferrand, France

Benjamin Rondeau
Laboratoire de Planétologie et Géodynamique
CNRS (Team 6112), University of Nantes, France

Emmanuel Fritsch

Update on sapphire mining in southern Madagascar. In July-August 2010, this contributor visited the Ilakaka-Sakaraha and Andranondambo mining areas in southern Madagascar with several companions (see listing at the end of this report). In addition to collecting reference samples for GIA, our goal was to assess the state of the sapphire industry in the region.

Discovered in 1998, the Ilakaka-Sakaraha deposit (figure 28) extends more than 80 km from the Isalo National Park toward Toliara on the southwest coast. It quickly became one of the world's most important gem deposits, producing an abundance of pink and blue sapphires. Although more than 99% of the blue sapphires require

Figure 29. These blue sapphires are from Andranondambo. Photo by V. Pardieu.

heat treatment to be marketable, several exceptional stones are found daily that do not require heating. The deposit also yields yellow, purple, violet, and pinkish orange "padparadscha" sapphires, as well as chrysoberyl (including alexandrite), zircon, garnet, spinel, and other gems. Mining takes place year-round, mostly by artisanal methods. Many dealers from Thailand and Sri Lanka continue to have buying offices in the area. Most purchases are exported to those two countries for heat treatment and cutting before the gems make their way to the market.

Gem mining in Madagascar, particularly in Ilakaka, has faced many difficulties in recent years. In particular, from February 2008 to July 2009, the Malagasy government banned all gem exports. Compared to previous visits in 2005 and 2008 by this author, the number of foreign buyers has clearly dropped, and digging in the Ilakaka area has waned. As a result, the mining community has suffered shortages of food and other necessities, and security issues are plaguing the region.

In 2010, we found only three small operations (two Thai, one Malagasy) still using machinery. Most of the companies once involved in mechanized mining have withdrawn because of the poor market, fuel costs, and a lack of support from the Malagasy authorities. Because the government tolerates illegal mining, it is very difficult for companies that own mining rights to work legally and responsibly.

At the time of our visit, the main mining area was located near Antsoa, a village on the Taheza River southeast of Sakaraha, where about 1,500 miners were backed by Sri Lankan and local buyers. Antsoa was reportedly producing the best blue sapphires, with fine rough stones up to 10 g. At the more than 20 other sites we visited, we found anywhere from 10 to 500 people working. We estimate that about 50,000 people are now earning a living (directly or indirectly) from sapphire mining in Ilakaka-Sakaraha, half the number reported in 2005.

In the Andranondambo area, blue sapphires are mined from several primary deposits. Société d'Investissement Australien à Madagascar, an Australian company, mined the area for a few years but stopped in 2009. Today, small groups of artisanal miners work sites near Andranondambo, Maromby, Tirimena, and Siva. The most active mining area appeared to be Ankazoabo (north of Andranondambo), where Malaysian company Nantin Ltd. was operating heavy machinery alongside some 200 artisanal miners using hand tools.

While many gems are still produced, particularly fine blue sapphires (e.g., figure 29), the shrinking margins have led to fierce competition between buyers. Meanwhile, the miners' living and working conditions are very difficult. Most mining companies have stopped their activities, and many buyers are considering a switch to ruby dealing in Mozambique.

The author thanks the following for helping with the expedition and editing this report: Nirina Rakotosaona (Société Minière du Cap, Antananarivo, Madagascar), Marc Noveraz (Switzerland), Richard W. Hughes (Bangkok), Tracy Lindwall (San Francisco), Lou Pierre Bryl (Gaspé, Canada), Jazmin Amira Weissgärber Crespo (Mannheim, Germany), and Philippe Ressigeac (Montauban, France).

Vincent Pardieu

A strongly thermoluminescent spodumene. Thermoluminescence is a property of some minerals whereby they glow when heated to a certain temperature. Minerals known to display this property include fluorite (referred to as chlorophane), apatite, calcite, lepidolite, and spodumene (see www.galleries.com/minerals/property/pleochro.htm#thermo). The Gem Testing Laboratory of Jaipur, India, recently examined a spodumene that showed a striking example of thermoluminescence.

The pear-shaped green stone (figure 30) weighed 16.17 ct and measured 19.94 × 11.55 × 10.82 mm. Its color was reminiscent of green beryl or emerald from Nigeria, but the bright luster and liveliness ruled out the possibility of beryl. The following gemological properties were recorded: RI—1.660–1.675; birefringence—0.15; hydrostatic SG—

Figure 30. This 16.17 ct green spodumene was notable for its strong thermoluminescence at low temperature. Photo by G. Choudhary.

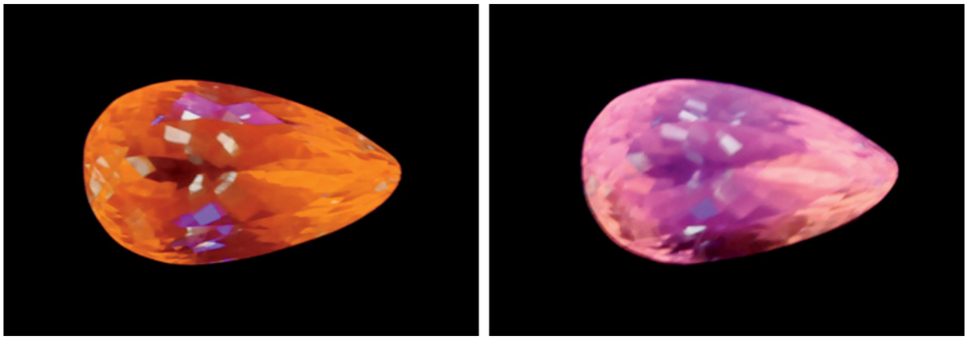

Figure 31. The spodumene in figure 30 fluoresced strong orange when exposed to long-wave UV radiation (left) and strong pink under short-wave UV (right). Photos by G. Choudhary.

3.17; fluorescence—strong orange to long-wave UV radiation and strong pink to short-wave UV (figure 31); and a weak absorption band visible in the blue region at around 440 nm in the desk-model spectroscope (no chromium lines were detected). These properties are consistent with those reported for spodumene (R. Webster, *Gems*, 5th ed., rev. by P. G. Read, Butterworth-Heinemann, Oxford, UK, 1994, pp. 186–189). With magnification, a few liquid "fingerprints" were observed under the table and crown facets. Cleavage planes, a common feature in spodumene, were not evident.

Microscopic examination was conducted with the aid of a fiber-optic lamp. Curiously, when the examination was completed, the green spodumene appeared bright orange (figure 32). Within a few minutes, however, the original green color returned. The orange glow was caused by the heat of the fiber-optic lamp exciting the spodumene's activator elements to produce thermoluminescence. The effect was similar to the stone's fluorescence reaction to long-wave UV radiation (again, see figure 31, left). The stone was reheated with the fiber-optic lamp and glowed orange again after three minutes of exposure, before returning to its original color within two to three minutes after removal of the lamp. These steps were repeated several times with consistent results.

EDXRF analysis revealed the presence of Al, Si, and Fe. Mn, a common constituent in spodumene that is also responsible for its strong fluorescence (see M. Robbins, *Fluorescence: Gems and Minerals Under Ultraviolet Light*, Geoscience Press, Arizona, 1994, pp. 265–266), was not detected in this specimen. Therefore, the cause of the fluorescence and thermoluminescence is unknown.

This is the first time this contributor has seen the heat of a fiber-optic lamp cause thermoluminescence in a gemstone. Webster (1994, p. 187) mentioned this effect occurring in X-ray irradiated kunzite at temperatures around 200°C. The present sample has probably not been laboratory irradiated, as the color was stable even after repeated heating with the fiber-optic lamp. Its thermoluminescence at such a low temperature makes it quite an unusual specimen.

Gagan Choudhary (gtl@gjepcindia.com)
Gem Testing Laboratory
Jaipur, India

"Neon" blue-to-green Cu- and Mn-bearing liddicoatite tourmaline. Four greenish blue faceted oval specimens, 1.29–1.45 ct, were recently submitted to the Gübelin Gem Lab (figure 33). The stones were similar in hue, tone, and saturation to Paraíba-type tourmaline. Standard gemologi-

Figure 32. The heat generated by a fiber-optic lamp caused the spodumene to thermoluminesce bright orange. The original green color returned within three minutes after the stone was removed from the lamp. Photo by G. Choudhary.

Figure 33. These four liddicoatite tourmalines (1.29–1.45 ct) have colors similar to those of some Paraíba-type elbaite tourmaline. Photo by L. Klemm.

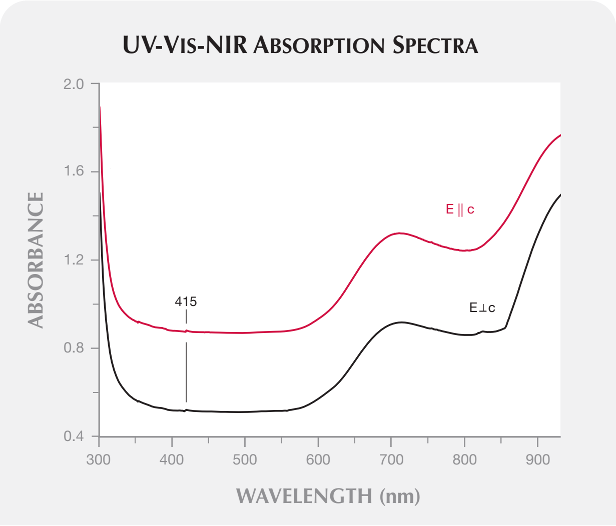

Figure 34. Polarized UV-Vis-NIR spectra of the stones in figure 33 show Cu^{2+} absorptions in the red region (~700 nm), with increasing absorption in the near-IR region (~900 nm). The small, sharp peak at ~415 nm is probably due to Mn^{2+}, and the increasing absorption toward the UV region is likely attributable to Mn^{2+}-Ti^{4+} intervalence charge transfer.

cal examination gave the following properties: RI—n_o = 1.640–1.641 and n_e = 1.621–1.622; birefringence—0.018–0.020; and SG—3.06–3.08; all these are consistent with tourmaline. Microscopic observation revealed parallel tubes, some hollow and others stained yellow to red-brown. Partially healed and unhealed fissures were also seen, and portions of the fissures were either frosted or reflective. Similar patterns have been observed in some heat-treated Paraíba-type tourmaline from Mozambique (B. M. Laurs et al., "Copper-bearing [Paraíba-type] tourmaline from Mozambique," Spring 2008 *G&G*, pp. 4–30). All four samples fluoresced moderate yellowish green to long-wave UV radiation and faint yellowish green to short-wave UV.

The samples' UV-Vis-NIR spectra (figure 34) were also similar to those of Paraíba-type tourmaline (see P. B. Merkel and C. M. Breeding, "Spectral differentiation between copper and iron colorants in gem tourmalines," Summer 2009 *G&G*, pp. 112–119, and references therein). Surprisingly, however, LA-ICP-MS analysis showed that though all of the samples were lithium tourmalines, they contained more Ca than alkalis (Na+K). EDXRF analysis also revealed significantly more Ca than typical of Paraíba-type tourmaline. All samples also contained minor amounts of Mn and Cu.

Elbaite is an Na-rich lithium tourmaline; the other lithium tourmalines are liddicoatite and rossmanite. Identification of tourmaline species is complex, as to date

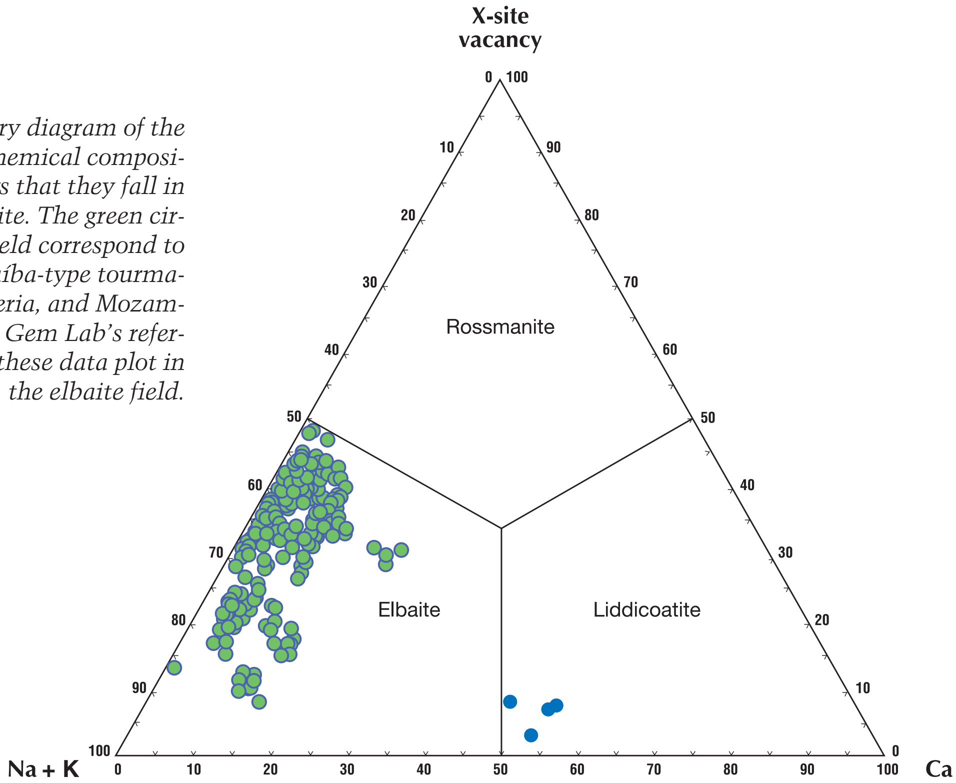

Figure 35. This ternary diagram of the four samples' average chemical composition (blue circles) shows that they fall in the field for liddicoatite. The green circles in the elbaite field correspond to analyses of typical Paraíba-type tourmaline from Brazil, Nigeria, and Mozambique in the Gübelin Gem Lab's reference collection; all of these data plot in the elbaite field.

there are 13 known end members. When plotting the chemical composition of these specimens on a ternary diagram for lithium-rich tourmaline, all four samples fell in the liddicoatite field (figure 35). Based on calculations using a recently developed tool (L. Klemm and P. Hardy, "Determination of tourmaline species by advanced chemical analysis," *Proceedings of the 3rd European Gemmological Symposium*, Berne, Switzerland, June 5–7, 2009, pp. 58–59) and averaging the four chemical analyses obtained on each stone by LA-ICP-MS, the samples contained a 50–57% liddicoatite component; thus, all four were liddicoatite tourmaline.

Some traders we spoke with believe that these stones are from Mozambique, near the mine that produced Paraíba-type elbaite. We also have been told that liddicoatite rough has been found in this area that does not need heat treatment to produce the desirable greenish blue coloration. This is the first report of Cu-Mn bearing liddicoatite tourmalines of such color.

Stefanos Karampelas (s.karampelas@gubelingemlab.ch)
and Leo Klemm
Gübelin Gem Lab, Lucerne, Switzerland

INSTRUMENTS AND TECHNIQUES

Use your LCD screen as a gemological tool. Most LCD (liquid crystal display) screens, such as those used for computer or mobile phone displays, are sources of plane-polarized light. We recently tested the possibility of using such screens to observe the pleochroism of faceted gems. When we placed a few gems table-down over the white portion of a mobile phone display, the pleochroism was readily visible (figure 36). Further, by using a handheld polarizer, such as a camera polarizing filter or even polarizing sunglasses, one can create a makeshift polariscope (figure 37).

Given the widespread use of LCD screens in various products, gemologists should keep them in mind as a convenient working tool when traditional instruments are not available, particularly in the field. Note, however, that some displays using new technology (e.g., OLED—organic light emitting diodes) are not a source of polarized light and thus cannot be used as gemological tools. It is therefore advisable to first test a screen with a polarizing filter.

Bertrand Devouard and Rémi Bornet
Laboratoire Magma et Volcans, Blaise Pascal University
CNRS (UMR 6524), Clermont-Ferrand, France

Franck Notari, Benjamin Rondeau,
and Emmanuel Fritsch

Smartphone photomicrography. Smartphones such as the Apple iPhone, Motorola Droid, and Nokia N8 have become increasingly popular in recent years. Top-end models typically feature good-quality digital cameras that rival some "point-and-shoot" cameras, in addition to having basic photo-editing software.

The popularity of smartphones has also spawned the development of numerous accessories that can expand their functionality even further. One such accessory is a low-power microscope that clips onto the phone over the camera lens. This contributor was interested in seeing if this device could have gemological applications.

The microscope accessory in figure 38 was ordered on the Internet for less than US$20. Its sliding housing offers varying levels of magnification, and illumination is provided by two white LEDs. The lighting assembly can be rotated about 45° to change the angle of illumination.

Although this device is clearly not optimized for gemological use, with some practice it was possible to produce serviceable photomicrographs. The images in figure 39 were taken with an Apple iPhone 4 using the ProCamera photography application, which allows manual adjustment of focus and white balance. As with any photogra-

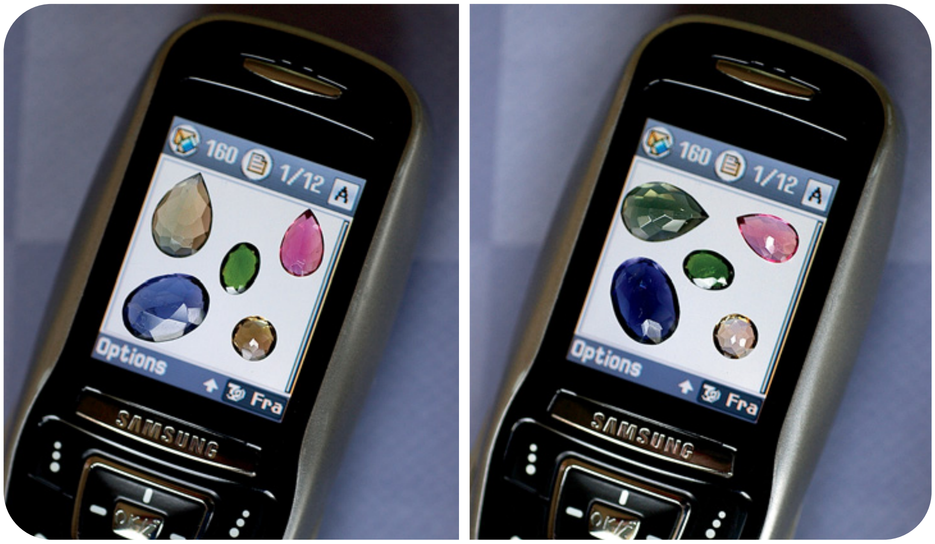

Figure 36. When pleochroic stones are placed table-down on an LCD screen, as on this cell phone, they display pleochroism when rotated 90° (from left to right and top to bottom: kornerupine, tourmaline, chrome diopside, iolite, and smoky quartz). Photo by B. Devouard.

Figure 37. A simple polariscope is created when a polarizer is placed in front of the plane-polarized LCD screen. Here, a colorless topaz has been rotated on the cell phone screen under a camera polarizing filter. Photo B. Devouard.

phy, the biggest challenge was the lighting. The LEDs proved too bright in most situations, and better results were achieved by partially shielding them or turning them off and relying on ambient light. Although the microscope's packaging promised magnification up to 60×, in practice it was impossible to obtain good focus beyond medium power (~20×). The best results were produced with a combination of the phone's digital zoom, careful adjustment of the autofocus, and a steady hand.

Figure 38. This inexpensive microscope accessory clips over a smartphone camera lens. Illumination is provided by LEDs. Photo by Robert Weldon.

Although this device clearly will not replace a standard gemological microscope or even a loupe, it appears to provide a useful field tool in the gemologist's arsenal.

Thomas W. Overton (toverton@gia.edu)
GIA, Carlsbad

SYNTHETICS AND SIMULANTS

Filled copal imitation of amber. Amber is one of the most popular gem materials for traditional Islamic prayer beads (*Mesbah* in Arabic). Specimens with inclusions of plants, insects, or even animals are often used. However, we have also seen amber imitations fashioned for this purpose.

We recently received a strand resembling amber that consisted of 33 yellow round beads (~12 mm in diameter) with two oval-shaped separators and a fancy-shaped link (figure 40). The round beads contained dark brown plant debris and a variety of insects: ants, mosquitoes, ladybugs, and flies, all in good condition. They were inert to short-wave UV radiation, but their reaction to long-wave UV was striking. They displayed a moderate chalky greenish yellow fluorescence, which appeared to be confined to the surface, together with distinctive chalky blue circular areas (figure 41)—most located near drill holes—that strongly suggested assemblages.

We obtained spot RI readings of 1.52 on the circular zones and 1.54 elsewhere. Observation between crossed polarizers revealed strong anomalous double refraction with

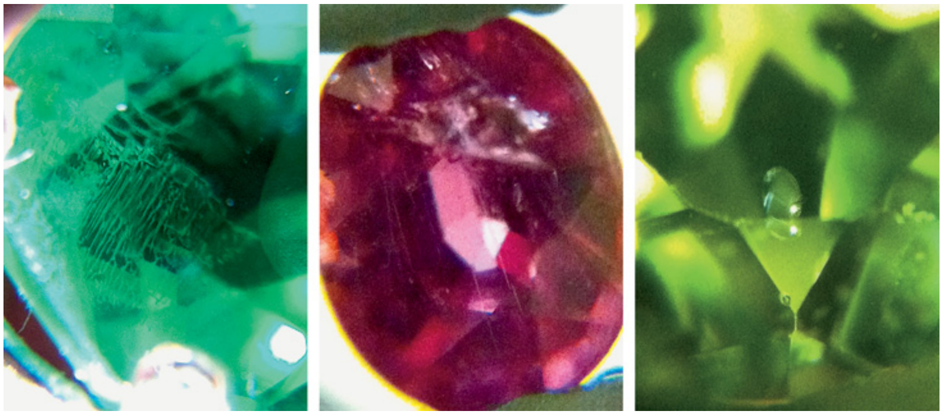

Figure 39. Taken with an Apple iPhone and the clip-on microscope in figure 38, these images show flux inclusions in synthetic emerald (left), needle-like inclusions in corundum, and a "lilypad" inclusion in peridot. Photomicrographs by T. W. Overton; fields of view ~4.0 mm.

strain colors. With the client's permission, we conducted hot-point and acetone tests on very small, inconspicuous areas. The main portion of the beads had a resinous odor, while the circular zones had an acrid odor. During acetone tests, the main areas revealed slightly softened and etched surfaces, while the circular portions showed even stronger surface etching. The characteristics of the bulk of the beads were consistent with copal, while those of the circular portions were consistent with plastic. This was the case for all 33 round beads, while the separators and link of the strand only showed characteristics consistent with copal, with no circular portions or insects.

Microscopic observation clearly revealed a separation plane between the main part of the beads and the circular blue-fluorescing areas, denoted by curved polish marks beneath the surface (figure 42, left). Examination with immersion (in water) indicated that all the round beads were cored and filled with a colorless to light yellow plastic, along with insects (figure 42, right). Gas bubbles were seen adjacent to insects within the plastic. In addition, a separation plane was visible between the beads' plastic core (containing the insects) and a plastic outer layer that formed the circular-fluorescing zones (which contained plant debris). The plant debris resembled that which was present in the copal, and apparently was added to the plastic to make it less noticeable.

On the basis of the evidence, we concluded that the beads consisted of copal filled with plastic to imitate insect-bearing amber. It appears that each round copal bead was subjected to the following process: (1) drilling

Figure 40. The beads in this rosary (~12 mm in diameter) proved to be copal filled and assembled with plastic to imitate amber. Photo by S. Singbamroong, © Dubai Central Laboratory.

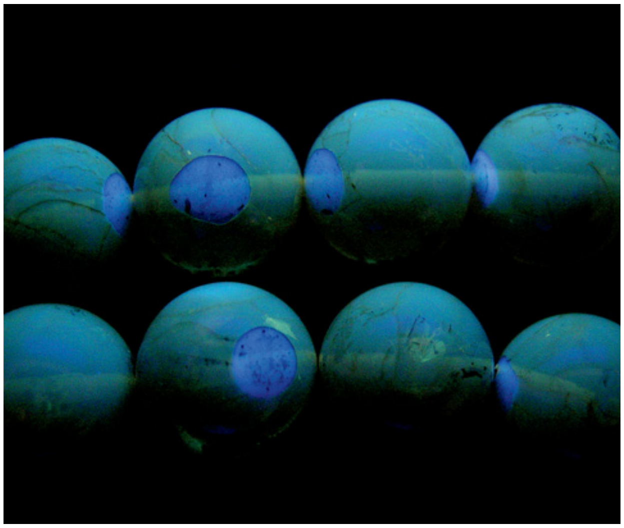

Figure 41. When exposed to long-wave UV radiation, the beads display a moderate chalky greenish yellow fluorescence, as well as chalky blue circular patterns. Photo by S. Singbamroong, © Dubai Central Laboratory.

and hollowing out the interior, (2) filling with plastic that contained insects, and (3) masking the hole with plastic containing plant debris. The inner filling material containing the insects was exposed on a small portion of the surface of a few beads, and acetone and hot-point testing of those areas gave results consistent with plastic.

Sutas Singbamroong (sssutas@dm.gov.ae) and
Moza Rashed Al Falasi
Gemstone Unit, Dubai Central Laboratory
Dubai, United Arab Emirates

Figure 42. Microscopic observation clearly reveals a separation plane between the main part of the beads and the blue-fluorescing round areas, denoted by circular polish marks beneath the surface (left). Immersion in water revealed they were copal beads that had been cored and filled with a colorless to light yellow material containing insects (right). Also visible are small bubbles next to the insect (white arrows) and a separation plane between the insect-bearing plastic in the core and an outer plastic layer containing plant debris (red arrows). Photomicrographs by S. Singbamroong, © Dubai Central Laboratory; magnified 10×.

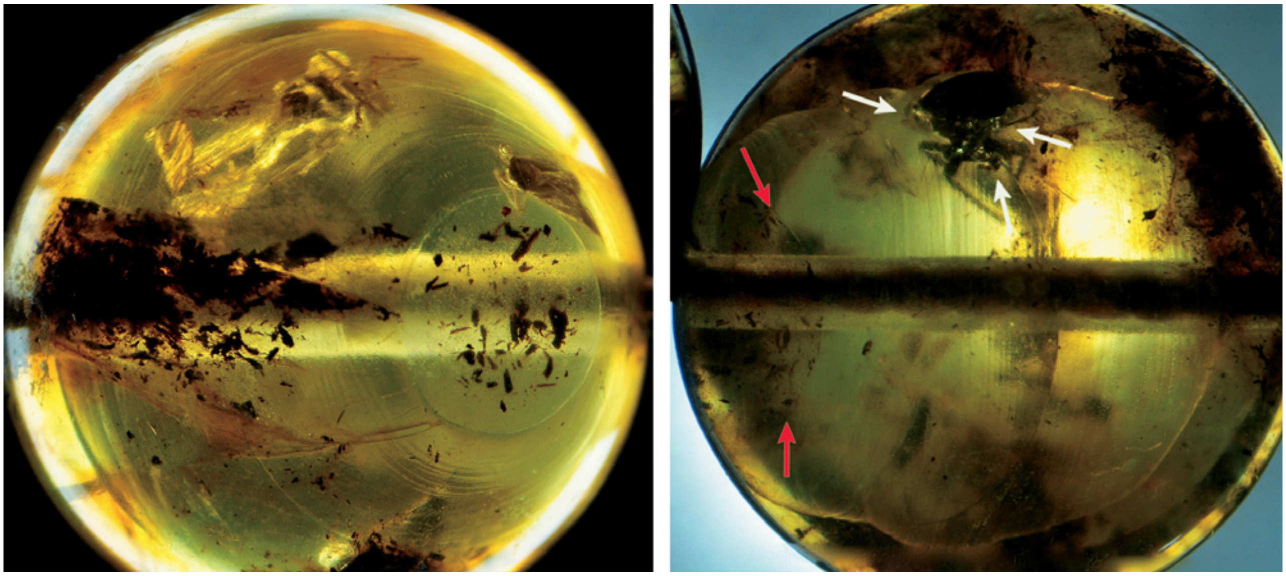

Glass with crystalline aggregates. Glass is the most common gem simulant and can show a wide variety of colors, transparencies, and optical effects. Most examples display similar features—namely gas bubbles, swirl marks, and devitrification effects—but in the last few years this contributor has encountered some interesting and unusual glass specimens (see, e.g., Summer 2007 GNI, pp. 174–175; Summer 2010 GNI, pp. 155–156).

Recently, the Gem Testing Laboratory of Jaipur, India, received a green 25.04 ct step cut measuring 20.04 × 14.86 × 6.36 mm (figure 43). It had the translucency of chalcedony and the color of emerald. None of emerald's distinct inclusions were observed microscopically, however, and the heft was sufficiently high to rule out emerald or chalcedony. Microscopic examination with fiber-optic light revealed aggregates of colorless crystalline features throughout the sample (figure 44). The crystals were easily resolved at higher magnification and were much larger than those found in cryptocrystalline materials such as chalcedony. The presence of these crystals initially suggested a natural origin.

Standard gemological testing, however, revealed the

Figure 43. This 25.04 ct translucent green specimen, which proved to be glass, is unusual for its crystalline features. Photo by G. Choudhary.

following properties: RI—1.745; hydrostatic SG—4.33; aggregate reaction in the polariscope; UV fluorescence—chalky blue to short-wave, and inert to long-wave UV. These properties indicated a glass, which was confirmed by FTIR and EDXRF analysis. The IR spectrum displayed twin humps between 3600 and 2600 cm^{-1} and complete absorption up to 2500 cm^{-1}, while qualitative EDXRF revealed the presence of Si, Ca, and Pb, the last being responsible for the high RI and SG values. During a subsequent microscopic examination of the sample, one gas bubble was finally resolved.

Crystalline features have been reported previously as inclusions in glass (see, e.g., H. A. Hänni et al., "A glass imitation of blue chalcedony," *Journal of Gemmology*, Vol. 27, No. 5, 2001, pp. 275–285; Lab Notes: Spring 2008, pp. 70–71; Summer 2010, pp. 144); these are attributed to partial devitrification. Hänni et al. (2001) identified the transparent and colorless crystalline inclusions as wollastonite, but those in our sample could not be identified with the techniques available.

Such specimens make very convincing gem simulants. In the absence of proper gemological testing and FTIR/EDXRF analysis, there is a strong possibility of misidentification.

Gagan Choudhary

Synthetic ruby specimen sold as natural. *G&G* has reported on a number of synthetic rubies sold as natural crystals (see Fall 1993 Lab Notes, p. 204; Fall 2001 GNI, pp. 243–245). A recent case underscores the importance of taking precautions against such frauds.

Dubai is a relatively new market for rough and polished colored stones, and an intersection between African sources and the Asian trade. It has also seen a variety of imitations of natural gem crystals. In fact, within the past two years, these contributors have reported on imitations of diamond and emerald crystals (Fall 2009 GNI, pp. 230–231; Winter 2009 GNI, pp. 305–306).

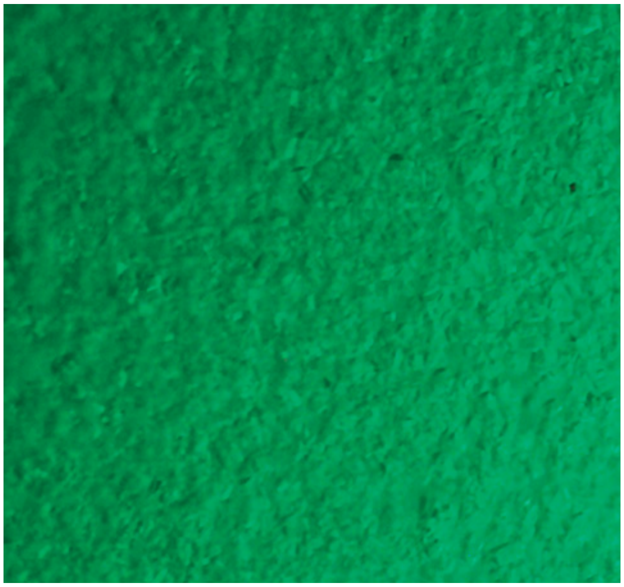

Figure 44. The glass specimen in figure 43 displays homogeneous colorless crystals throughout, giving it an aggregate structure. Photomicrograph by G. Choudhary; magnified 60×.

Recently, the Dubai Central Laboratory received a rough specimen for identification. The red "crystal" (figure 45) had a distorted hexagonal shape and was attached to some matrix material. It was identified as ruby by its absorption spectrum with a handheld spectroscope, a finding confirmed by UV-Vis-NIR spectroscopy. Using a microscope, we observed curved striae and filled cavities; gas bubbles were visible in the filling material. We therefore identified this sample as synthetic ruby with filled fractures. Raman spectroscopy identified the matrix as quartz, which had been joined to the synthetic ruby by some type of glue. Since quartz is geologically incompatible with corundum, the matrix provided another clue that this specimen was a fake.

This case again illustrates the importance of gem laboratory reports and the necessity of thoroughly examining a piece before purchase.

Nazar Ahmed (nanezar@dm.gov.ae)
and Hassan Al Marzooqi
Gemstone Unit, Dubai Central Laboratory
Dubai, United Arab Emirates

MISCELLANEOUS

Louis XV's Golden Fleece—recreated. In 1743, King Louis XV of France became a knight of the Order of the Golden

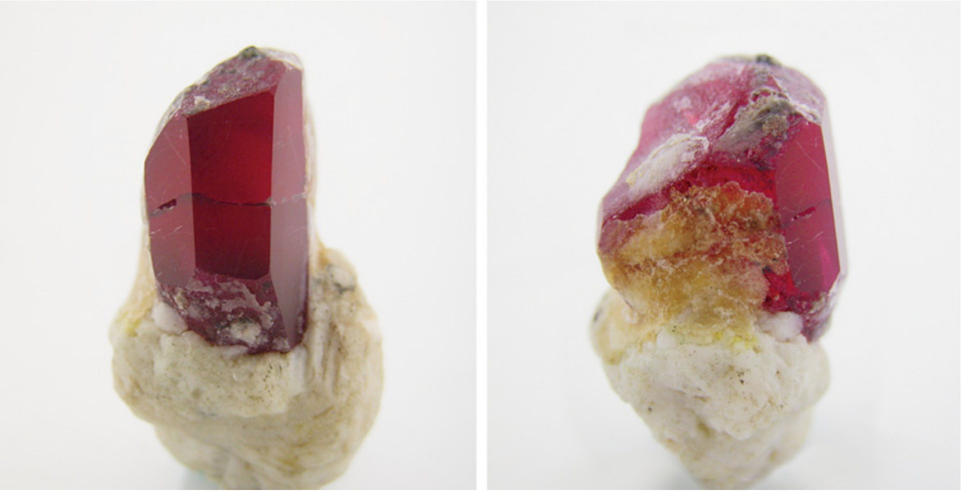

Figure 45. This synthetic ruby "crystal" (2.7 cm tall) was fashioned to imitate natural ruby in matrix. Photos by N. Ahmed, © Dubai Gemstone Laboratory.

Fleece, the first French ruler to receive this distinction since its founding in Burgundy three centuries earlier. In 1749, the king's jeweler, Jacqumin, created an emblem of this order for the king. It was composed of three exceptional gems: the 69 ct French Blue diamond; a 32.62 ct light blue diamond later named the Bazu; and the 107 ct Côte de Bretagne, a spinel carved as a dragon. This masterpiece of French rococo jewelry was stolen and disassembled in 1792 during the revolution; only the spinel carving remained intact, and it now resides in the Louvre. Many historians have since tried to reconstruct this emblem on paper (e.g., B. Morel, *The French Crown Jewels*, Fonds Mercator, Antwerp, 1988; H. Tillander, *Diamond Cuts in Historic Jewelry: 1381–1910*, Art Books Intl. Ltd., London, 1995).

Recently, these contributors recreated the Golden Fleece as accurately as possible, based on a 2008 painting (see figure 15 in Farges et al., "The French Blue and the Hope: New data from the discovery of a historical lead cast," Spring 2009 *G&G*, pp. 2–17) as well as a drawing of the original piece that was discovered in the 1980s in Switzerland. We tried to incorporate Jacqumin's techniques and *savoir faire* by using 3D rendering for the design and analyzing historical elements (such as diamond setting) that were not available to, or not considered by, previous investigators.

Replicas of the two blue diamonds were created from cubic zirconia. The Côte de Bretagne dragon was carved from lead glass using a wax replica based on 3D-scaled pictures of the original. Gold and manganese pigments in the glass were used to simulate the color of the spinel. The emblem's 500+ remaining "diamonds" were fashioned from cubic zirconia using a baroque cushion cut. The red and yellow stones, which adorned the dragon's flames and the golden fleece, were made from colorless CZ and then painted on their backs, following Jacqumin's original method.

Since the emblem was most likely made of silver-plated gold, as was the custom for French royal jewelry at the time (the setting of diamonds in gold was considered tasteless by royal French jewelers), we decided to create a setting constructed primarily of sterling silver. The metal was carved to recreate the delicate distribution of the dragon's wings and tail, as well as the palms over which the dragon is suspended. Some parts of the silver setting were gilded to recreate the elegant combination of gold and silver that likely prevailed in the original, and all the stones were set using 18th century techniques.

After three years of work, the recreated Golden Fleece (figure 46) was unveiled on June 30, 2010, at the site where the original jewel was stolen in 1792: the former royal storehouse, now the Hôtel de la Marine on Place de la Concorde in Paris. The event was filmed for a documentary on the French Blue, and an English-language version titled "Secrets of the Hope Diamond" will be broadcast in the U.S. in 2011 on the National Geographic channel.

Herbert Horovitz
Geneva, Switzerland

François Farges (farges@mnhn.fr)
Muséum National d'Histoire Naturelle
Paris, France

CONFERENCE REPORTS

20th Annual Goldschmidt Conference. The geochemistry-focused Goldschmidt Conference was held June 13–18, 2010, in Knoxville, Tennessee. The meeting featured a session titled "Geochemistry and Trace Elements in Gem Materials," chaired by **Drs. Emmanuel Fritsch** and **Benjamin Rondeau** (both from the University of Nantes, France), who opened with a brief discussion on the increasing importance of trace-element chemistry for investigating gemological problems. Their remarks were followed by several interesting talks. Abstracts can be viewed at www.goldschmidt2010.org/abstracts/view.

This contributor demonstrated the use of LA-ICP-MS analysis in separating amethyst, citrine, and malachite from their laboratory-grown equivalents. **Dr. Adolf Peretti** (GRS Gemresearch Swisslab, Lucerne) presented data showing small-scale chemical variations within single

Figure 46. This photo of the reconstructed Golden Fleece (~16 × 5 cm) shows a CZ replica of the 69 ct French Blue that is set above the fleece composed of about one hundred yellow paint–backed cubic zirconias, and set below a glass replica of the 107 ct Côte de Bretagne spinel. Photo by F. Farges.

crystals of Paraíba-type tourmaline, and cautioned against using color-specific geochemical criteria to identify geographic origin. **Dr. Laurence Galoisy** (University of Paris) discussed the role of chromium and other transition elements in the color of garnets from Thailand and East Africa. **Kaifan Hu** (Pennsylvania State University, University Park) showed how gem pietersite from Namibia can be separated from similar Chinese material on the basis of microstructures.

Both session leaders examined the chemical composition of opal. **Dr. Fritsch** described how differences in uranium content affect the occurrence of green and blue UV luminescence. **Dr. Rondeau** presented geochemical data for opals from Wollo, Ethiopia (see Summer 2010 *G&G*, pp. 90–105). Of particular note were elevated barium concentrations, which are atypical of opal from volcanic environments.

Two talks dealt with trace elements in diamond. **Yakov Weiss** (Hebrew University of Jerusalem) categorized the trace-element composition of fluids trapped in fibrous diamonds into three groups that might prove useful in determining geographic origin. **Dr. Eloïse Gaillou** (Smithsonian Institution, Washington, DC) set forth a method for calculating total boron concentration in type IIb blue diamonds and compared that with existing methods using FTIR analysis.

Three posters also were displayed as part of the gem session. **W. Bieri** (GRS Gemresearch Swisslab) showed how the chemical composition of apatite inclusions in corundum and spinel can help specify the geographic origin of the host gem. **Dr. Andy H. Shen** (GIA Laboratory, Carlsbad) presented detailed data showing the possibility of using LA-ICP-MS analysis to measure trace concentrations of silicon in sapphire; this element may have an important effect on color centers in corundum. Finally, **Kristen Yetter** (New Mexico State University, Las Cruces) showed how LIBS analysis can provide a preliminary indication of geographic origin in some rubies and sapphires.

Christopher M. Breeding (mbreedin@gia.edu)
GIA Laboratory, Carlsbad

20th General Meeting of the International Mineralogical Association (IMA). This meeting was held August 21–27 at Eötvös Lorand University in Budapest. Some 1,700 participants from 74 countries attended, making it the largest IMA event to date. The conference featured several presentations of gemological interest, some of which are summarized here. Abstracts of all oral and poster presentations can be found at www.ima2010.hu/img/doc/ima2010_abstracts.pdf.

In an invited presentation, **Thomas Hainschwang** (Gemlab Laboratory, Balzers, Liechtenstein) reviewed the challenges of separating natural- and treated-color diamonds using visible, infrared, and photoluminescence spectroscopy. These techniques allow researchers to characterize optical defects in diamonds, some of which can be created, modified, or destroyed by laboratory treatment processes. The behavior of optical defects during treatment is a key to colored diamond identification. **Dr. Thomas Stachel** (University of Alberta, Edmonton, Canada) showed that most gem diamonds originate from several source rocks in portions of the lithospheric mantle beneath cratons. **Dr. Richard Taylor** (University of Saint Andrews, Scotland) discussed the chemical analysis of trace elements in gem feldspars using two analytical techniques: X-ray absorption fine structure (XAFS) and X-ray excited optical luminescence (XEOL). **Dr. Alessandra Costanzo** (National University of Ireland, Galway) described the results of a study of fluid inclusions in emeralds from the Piteiras mine in Minas Gerais, Brazil. **Dr. Bertrand Devouard** (Blaise Pascal University, Clermont-Ferrand, France) presented detailed chemical composition data on pezzottaite samples from Madagascar, Afghanistan, and Myanmar. Some specimens from Myanmar displayed hourglass-shaped color zoning, with significantly greater cesium content in the more strongly colored sectors.

One of these contributors (SK) compared microradiography with X-ray computed microtomography for imaging the internal structure of pearls. Despite a data-collection time lasting several hours, computed microtomography offered improved resolution over conventional imaging techniques. A study of the internal features and chemical composition of 170 alexandrite samples from various sources was presented by **Anna-Kathrin Malsy** (Gübelin Gem Lab, Lucerne, Switzerland). On the basis of LA-ICP-MS analyses, most sources could be differentiated on a triangular plot of boron, tin, and magnesium contents. The chemical composition data proved far more valuable than microscopic examination, since there were no diagnostic inclusions.

Dr. Pornsawat Wathanakul (Kasetsart University, Bangkok) compared the properties of blue-green-yellow sapphires from the Nam Khun–Nam Yuen region of Thailand and Garba Tula in Kenya. Both groups of sapphires come from basaltic host rocks, but slight differences in their visible absorption spectra appear to distinguish them. **Somruedee Satitkune**, also of Kasetsart University, examined mineral inclusions in diamonds from the Koffiefontein and Finsch mines in South Africa. She showed that inclusions with cubic symmetry (such as pyrope and chromite) exhibit nearly the same angular orientation to the {111} crystal face of diamond, whereas inclusions of minerals with lower symmetry (diopside and olivine) display more variable angular orientations.

Dr. Gaston Giuliani (Institute of Research for Development, and Center for Petrographic and Geochemical Research, Nancy, France) described how metamorphism of evaporates associated with sedimentary carbonate rocks provided the fluids partly responsible for the formation of some important colored stone deposits. **Dr. Dorrit Jacob** (Johannes Gutenberg University, Mainz, Germany) detailed the use of chemical composition data obtained by LA-ICP-MS analysis to differentiate freshwater cultured pearls from various geographic sources using the ratio of Ba/Sr versus B concentrations. **Tashia Dzikowski** (University of British Columbia, Vancouver, Canada) reported on the discovery of a ruby and sapphire deposit hosted in marbles near Revelstoke, British Columbia. She also provided details on the geologic conditions of corundum formation. **Dr. Tobias Häger** (Johannes Gutenberg University) described an interesting occurrence of ruby and sapphire, rimmed by spinel, from the Luc Yen–Yen Bai mining area in Vietnam. Microscopic evidence suggests the spinel formed by an alteration reaction between corundum and dolomite.

During the conference, a meeting of the IMA Commission on Gem Materials (CGM) was held under the direction of the chair of the commission, **Dr. Lee Groat** (University of British Columbia, Vancouver). Among the items discussed was the creation of a CGM website, which may include an online atlas of gem deposits and also links to gem museums throughout the world.

James E. Shigley (jshigley@gia.edu)
GIA Research, Carlsbad
Stefanos Karampelas

Carpathian and Balkan Geological Association (CBGA) meeting. The 19th meeting of the CBGA took place in Thessaloniki, Greece, August 23–26, 2010. About 700 participants from 15 countries attended the event, which for the first time featured a session on gemology, with a particular focus on archeogemology as well as gems from the Carpathian and Balkan regions.

In the keynote lecture, **Dr. Emmanuel Fritsch** (University of Nantes, France) gave an update on the origin of color in minerals and gems. **This contributor** presented a nondestructive study of four late-16th and early-17th century religious artifacts from the Benedictine Abbey of Einsiedeln, Switzerland. The results of this analysis were compared with observations recorded at the end of the 17th century (for more details, see the article on pp. 292–296 of this issue).

Elisabeth Strack (Gemmological Institute of Hamburg, Germany) used "classical gemology" to investigate three jewelry pieces uncovered from the ruins at Veliki Preslav, Bulgaria, that date from the 9th century. These items contained a garnet, purple sapphires, emeralds with indications of Egyptian origin, and saltwater pearls. **Dr. Corina Ionescu** (Babes-Bolyai University, Cluj-Napoca, Romania) examined some unusual 5th century garnet-set jewelry (see the GNI entry on pp. 316–318 of this issue). A report on Bulgarian gem carvings from the Neolithic and Chalcolithic periods and their impact on the history of gemology was presented by **Dr. Ruslan I. Kostov** (St. Ivan Rilski University of Mining and Geology, Sofia). He indicated that these carvings represent the earliest record of fashioned nephrite from Bulgaria (figure 47) and the earliest known turquoise from the eastern Rhodope Mountains.

In the poster session, **Zoran Miladinović** (University of Belgrade, Serbia) discussed some deposits of gem-quality silica minerals (e.g., amethyst) found in a volcanic complex extending from southern Serbia to northern Greece (the Lece-Chalkidiki metallogenic zone). **Dr. Ludmila Illašová** (Constantine the Philosopher University, Nitra, Slovakia) reviewed opals and other gem-quality silica minerals from various locations in Slovakia. **Dr. Magdalena Dumańska-Słowik** (University of Krakow, Poland) offered preliminary results from a fluid inclusion study of topaz crystals from Volodarsk-Volynski, Ukraine, that apparently formed at about 360–385°C. Preliminary results from an FTIR and powder X-ray diffraction study of heated and unheated freshwater cultured pearls were presented by **Eleni Theodosoglou** (Aristotle University of Thessaloniki, Greece). Color differences were observed after heating at 250°C for one hour in air (5°C/min heating rate). The samples' XRD patterns did not change after heating, but some infrared bands showed slight differences related to organic matter and water.

Figure 47. This zoomorphic nephrite amulet from Bulgaria measures 4.2 × 3.7 cm and is from the early Neolithic period (i.e., end of the 7th millennium BC). Courtesy of the Regional Historical Museum, Kurdjali, Bulgaria (collection no. 4532); photo by Vladimir Alexeev.

The 20th CBGA meeting will take place in Albania in 2014.

Stefanos Karampelas

European Diamond Conference. More than 300 delegates attended the 21st European Conference on Diamond, Diamond-Like Materials, Carbon Nanotubes, and Nitrides, held September 5–9, 2010, in Budapest. Highlights of gemological interest from the ~330 oral and poster presentations are summarized here.

Several researchers, including **Dr. Mikhail Lukin** (Harvard University) and **Dr. Mark Newton** (University of Warwick, England) presented new research on nitrogen vacancy (NV) centers that occur—or have been created after growth—in synthetic diamond. NV centers are common in natural diamonds as well, and have proven important for the detection of HPHT treatment since the late 1990s.

Dr. Bert Willems (HRD, Antwerp) presented a study of six CVD synthetic diamond samples grown at LIMHP-CNRS (Villetaneuse, France). These high-quality plates contained varying nitrogen contents (up to 200 ppm) and were characterized by a 525 nm band in the UV-Vis absorption spectra, along with strong NV centers and a silicon peak at 737 nm.

Dr. Riadh Issaoui (LIMHP-CNRS) provided the latest results of growing free-standing type IIb CVD synthetic diamond plates. Good-quality plates (measuring 5 × 5 mm and 200 μm thick) were grown at an intermediate microwave power density of 80 W/cm^3, a substrate surface temperature of 800–1000°C, a total feed-gas rate of 200 standard cubic centimeters per minute, a boron-to-carbon ratio of 3000 ppm, and a 5% methane concentration.

Dr. Andrey Bolshakov (Russian Academy of Sciences, Moscow) grew thin films of CVD synthetic diamond that mimicked the structure of opal, resulting in novel three-dimensional photonic crystals. Using porous synthetic opal as a template, he and his colleagues grew CVD synthetic diamond either in the voids between the silica spheres or in place of the etched silica. With the recent interest in diamond-like coatings applied to gemstones, the implications of this work may someday be seen in the jewelry industry.

This contributor compared the phosphorescence spectra results of 357 natural type IIb diamonds with those of HPHT-treated and HPHT-grown synthetic diamonds. The only phosphorescence bands observed in the natural diamonds were centered at 500 and 660 nm. None of the treated or synthetic diamonds showed the 660 nm band, but all did display the 500 nm band, usually at higher intensity than in the comparable natural diamonds.

Sally Eaton-Magaña (smagana@gia.edu)
GIA Laboratory, Carlsbad

5th International Workshop on Provenance and Properties of Gems and Geo-materials. Since 1997, these workshops have been held approximately every two years in Hanoi. The most recent session took place October 18–24, 2010, at the Vietnamese Academy of Science and Technology, with more than 60 participants from 13 countries in attendance. The workshop started with a one-day field trip to an akoya pearl farm at Ha Long Bay (figure 48). Over the next three days, about 40 talks and posters were presented.

Dr. Christoph Hauzenberger (University of Graz, Austria) discussed the petrology and geochemical characteristics of spinel rims surrounding some ruby and sapphire samples from Truc Lau in northern Vietnam. **Dr. Chakkapan Sutthirat** (Gem and Jewelry Institute of Thailand and Chulalongkorn University, Bangkok) compared the spectroscopic, chemical, and microscopic characteristics of Vietnamese rubies from two different regions, Luc Yen and Quy Chau. **Dr. Visut Pisutha-Arnond**, representing the same institutions as Dr. Sutthirat, gave an update on the spectroscopic, chemical, and microscopic characteristics of gem-quality purplish red almandine from Houaphan Province in northeastern Laos. **Dr. Pornsawat Wathanakul** (Gem and Jewelry Institute of Thailand and Kasetsart University, Bangkok) offered preliminary means of identifying the origin of some alexandrites. **Walter Balmer** (Chulalongkorn University) delivered a portion of his Ph.D. research on the possible genetic link between the marble-hosted ruby deposits in Luc Yen and those near Yuan Jiang in the Ailao Shan Mountains of China.

Dr. Boontawee Sriprasert (Department of Mineral Resources, Bangkok) summarized heating experiments on the coloration of tourmaline. **Dr. Bhuwadol Wanthanachaisaeng** (Burapha University, Chanthaburi, Thailand) outlined the identification of heat-treated zircons by their FTIR spectra. **Dr. Kanphot Thongcham** (Ramkhamhaeng University, Bangkok) examined the effects of annealing on the color of zircon. **Dr. Vu Phi Tuyen** (Vietnamese Academy of Science and Technology, Hanoi) presented the results of photoluminescence and thermoluminescence studies of zircon during annealing.

Dr. Tobias Häger (Johannes Gutenberg University, Mainz, Germany) described gemological applications of Cr^{3+} luminescence. In some spinels, Dr. Häger reported, the FWHM (full width at half maximum) of chromium bands at ~700 nm increases after heat treatment. **Dr. Lutz Nasdala** (University of Vienna, Austria) described defect luminescence of ion-irradiated gem materials, focusing on diamond and zircon.

One of these contributors (SK) described the structures and pigments observed in natural pearls, focusing on non-nacreous types such as melo, scallop, and quahog. **Dr. Jayshree Panjikar** (Institute of Gem & Jewellery, Pune, India) reviewed the microscopic and crystallographic features of gem-quality beryl from India.

The last day of the presentations took place at the headquarters of Doji Gold & Gems Group, where participants were briefed on the company's gem mining activities and their cutting factory. In addition, **Dr. Dietmar Schwarz** (Gübelin Gem Laboratory, Lucerne, Switzerland) reviewed ruby, sapphire, and emerald mining and marketing. The conference closed with a three-day field trip, led by Doji vice chairman **Duong Anh Tuan**, to a primary marble-hosted spinel mine and a secondary ruby and spinel mine in the Yen Bai region.

Stefanos Karampelas

Le Thi-Thu Huong
Faculty of Geology, Vietnam National University
Hanoi

Figure 48. This akoya cultured pearl farm is located at Ha Long Bay in northeastern Vietnam. Photo by Christoph Hauzenberger.

ERRATA

1. The Summer 2008 GNI section (pp. 184–185) erroneously reported the yellow vanadinite locality as the Democratic Republic of the Congo. Dr. Lavinsky's supplier has now admitted that the material was actually found in Otjitheka, Kaokoland, northwest Namibia.

2. The business retrospective article by R. Shor and R. Weldon in the Fall 2010 issue (pp. 166–187) incorrectly stated that the American Gem Society Laboratory was the first grading lab to issue a cut grade on diamond grading reports. A number of smaller labs were in fact issuing cut grades prior to AGS. We thank David Atlas for bringing this to our attention.

3. There were two errors in table 1 of the gem localities retrospective article by J. E. Shigley et al. in the Fall 2010 issue (pp. 188–216). On page 203, the Hiddenite emerald locality is located in Alexander County, not Mitchell County. On page 214, Malawi should not have been listed as a tourmaline locality; the Canary deposit is actually located in Lundazi, Zambia.

4. The C. M. Breeding et al. technology retrospective article in the Fall 2010 issue (pp. 241–257) incorrectly referred to the Holloway Cut Adviser as Holloway Cut Analysis. In addition, The Lexus M-Box software referred to in the article was developed by OctoNus (Lexus is the distributor) and the image in figure 10 shows the Oxygen software user interface. The rough diamond planning system also makes use of DiamCalc, which OctoNus developed in the late 1990s and today is used widely to assist in the evaluation of diamond cutting. Our thanks to Sergey Sivovolenko for providing this additional information.